A Kinetic Model to Evaluate Cholesterol Efflux from THP-1 Macrophages to Apolipoprotein A-1†

Katharina Gaus,*,‡ J. Justin Gooding,§ Roger T. Dean,‡ Leonard Kritharides,⊥,|| and Wendy Jessup‡

Cell Biology Group and Clinical Research Group, Heart Research Institute, 145 Missenden Rd, Camperdown 2050, NSW, Australia, School of Chemistry, The University of New South Wales, Sydney 2052, NSW, Australia, and Department of Cardiology, Concord Hospital, NSW, Australia

Received February 15, 2001; Revised Manuscript Received May 11, 2001

ABSTRACT: The kinetics (0 to 3 h) of cholesterol efflux to delipidated apolipoprotein A-1 were investigated, and the experimental data were best fitted to a mathematical model that involves two independent pathways of cholesterol efflux. The first pathway with a rate constant of 4.6 h^{-1} is fast but removes only 3−5% of total cholesterol. After preconditioning apoA-1, it was found that this pathway remains, and hence it is a property of the cholesterol-loaded cells rather than due to modification on the apolipoprotein. This fast initial efflux does not seem to contribute to cholesterol efflux at later stages (>1 h) where a second pathway predominates. However, the fast initial efflux pool can be restored if apoA-1 is withdrawn. The second slower pathway ($k_{membrane-media} = 0.79\ h^{-1}$) is associated with cholesterol ester hydrolysis whose rate constant could be experimentally verified ($k_{cal} = 0.43$, $k_{exp} = 0.38 \pm 0.05$). The model suggests that two different plasma membrane domains are involved in the two pathways. Loading of the cells with an oxysterol, 7-ketocholesterol (7K), inhibits efflux from both pathways. The model predicts that 7K decreases the initial efflux by decreasing the available cholesterol (by possibly affecting lipid packing), while all rate constants in the second pathway are decreased. In conclusion, the kinetic model suggests that cholesterol efflux to apoA-1 is a two-step process. In the first step, some of the plasma membrane cholesterol contributes to a fast initial efflux (possibly from lipid rafts) and leads to a second pathway that mobilizes intracellular cholesterol mobilization.

The association of oxidized forms of cholesterol, oxysterols, with atherogenesis has been studied since the identification of such compounds in human atherosclerotic plaques (*1*, *2*). Of particular interest is the finding that oxysterols can contribute to foam cell formation by inhibiting reverse cholesterol transport (*3*, *4*). Our group has previously shown that macrophages enriched with 7-ketocholesterol (7K),[1] one of the major oxysterols found in plaques, have impaired cholesterol efflux to lipid-poor apolipoprotein A-1 (apoA-1) (*5*) but not to phospholipid-containing apoA-1 disks (*6*). This observation supports the hypothesis that cholesterol efflux and its mechanism is dependent on the nature of the extracellular cholesterol acceptor (*7*, *8*).

It is generally accepted that there are at least two pathways by which cholesterol can be removed from peripheral cells. Cholesterol acceptors which already contain phospholipids, such as HDL particles or PL-apoA-1 disks, can remove cholesterol by diffusion via a concentration gradient between the membrane cholesterol donor and acceptor particle (*9*). The aqueous diffusion model is therefore a bi-directional mass transport model which does not require the acceptor particle to bind or penetrate the cellular plasma membrane (*10*, *11*). The level of expression of the scavenger receptor B type 1 (SR-B1) is correlated with rates of cholesterol efflux to HDL or phospholipid particles (*12*). The ability of SR-B1 to stimulate cholesterol efflux appears independent of receptor−ligand binding and may reflect effects on the organization of membrane cholesterol domains that facilitate aqueous diffusion of cholesterol to acceptor particles (*13*).

Alternatively, lipid-poor cholesterol acceptors such as apoA-1 interact directly with the plasma membrane (*14*, *15*), simultaneously abstracting both cholesterol and phospholipid. Cholesterol efflux to lipid-free apoA-1 is largely dependent on expression of the ATP binding cassette transporter A1 (ABCA1). While its importance in apoA-1 mediated cholesterol efflux is clear, the exact function of ABCA1 in cholesterol export remains controversial, with recent studies suggesting roles as an apoA-1 receptor, an intracellular cholesterol transporter or in inducing modifications to membrane lipid distribution that favor apoA-1 docking at the cell surface (*16*−*18*).

† KG would like to acknowledge financial support from BASF and Studienstiftung des deutschen Volkes. This work was also supported by the National Health and Medical Research Council of Australia (NHMRC Project Grant 11920 to W.J. and L.K. and a NHMRC Principal Research Fellowship to W.J.).

* To whom correspondence should be addressed. Ph: 61-2-9550 3560. Fax: 61-2-9550 3302. E-mail: k.gaus@hri.org.au.

‡ Cell Biology Group, Heart Research Institute.

§ The University of New South Wales.

⊥ Clinical Research Group, Heart Research Institute.

|| Concord Hospital.

[1] Abbreviations: 7K, 7-ketocholesterol; 7KAcLDL, 7K-enriched AcLDL; 7KE, 7K esters; ACAT, acyl-CoA: cholesterol acyltransferase; AcLDL, acetylated LDL; apoA-1, apolipoprotein A-1; cal, calculated; CH, cholesterol; CE, cholesterol esters; EDTA, ethylenediaminetetraacetic acid; ERF, error function; exp, experimental; FBS, fetal bovine serum; LDL, low-density lipoprotein; obs, observed; PBS, phosphate-buffered saline; PMA, phorbol-12-myristate-13-acetate.

10.1021/bi010323n CCC: $20.00
Published on Web 07/31/2001

In this study, we investigate the kinetics of cholesterol removal to delipidated apoA-1 and the inhibitory effect of 7K on this system. Previously, kinetic studies were useful in the characterization of pathways of cholesterol removal and elucidation of intracellular cholesterol distribution stimulated by various acceptors (reviewed in (*9*)). Cholesterol efflux was observed to be nonlinear, and a mathematical model was established to interpret the data and extract rate constants. Morel et al. have applied a similar approach to cholesterol efflux from 25-hydroxycholesterol-enriched macrophages to both HDL and albumin and have found that this oxysterol increased the rate constant for both ester hydrolysis and esterification as well as those for bi-directional movement between the plasma membrane and the extracellular media (*19*). Alternative models with "two pools" accessible for cholesterol efflux have also been defined for efflux to lipidated apolipoproteins (*10*, *20*) and to lipid-free apoA-1 as well as HDL (*21*). These established models are discussed but cannot be adequately fitted to the kinetic data for efflux to lipid-free apoA-1 that we observed in the present study.

We suggest a model that comprises two parallel pathways with different kinetics. Additionally, we present experimental data indicating that two different plasma membrane domains are involved in these two pathways and suggest that the initial pathway is necessary to stimulate the second pathway.

METHODS

Materials. All chemicals were of analytical grade and all solvents were HPLC grade (Mallinckrodt). Bovine serum albumin (BSA, essentially fatty acid free), Dulbecco's phosphate buffered saline (PBS), chloramphenicol, EDTA, PMA, and cholesterol were purchased from Sigma. 7-ketocholesterol (7K) was obtained from Steraloids Inc. ^{3}H-cholesterol (1 μCi/μL) was obtained from Amersham. RPMI (Trace Biosciences) was supplemented with 2 mM L-glutamine (Trace Biosciences) and penicillin/streptomycin (100 U/100 μg in 1 mL, Sigma) at the time of use. Heat-inactivated fetal bovine serum (FBS) was purchased from Trace Bioscience. Acyl-CoA:cholesterol acyltransferase (ACAT) inhibitor was Sandoz S-58035 (3-[decyldimethylsilyl]-*N*-[2-(4-methylphenyl)-1-phenylethyl]propanamide) and was a gift from Sandoz Inc.

Lipoprotein Preparation and Acetylation. Incorporation of 7K into lipoproteins, LDL isolation and modification have been described previously (*5*). In brief, plasma from fasted normolipidemic subjects was collected, anti-coagulated with 2mM EDTA, and incubated with a small volume of an ethanolic solution of 7K (final 7K concentration 2.5 mM; final ethanol concentration 2% v/v) for 6 h at 37 °C with gentle shaking. The 7K-enriched LDL (7KLDL) or native LDL (density: 1.021−1.063) were isolated by density gradient ultracentrifugation, dialyzed against deoxygenated PBS containing EDTA (1 g/L) and chloramphenicol (0.1 g/L), and filter-sterilized (0.45 μM). LDL and 7KLDL were acetylated as described previously (*4*). EDTA was removed by gel filtration (PD10 columns, Pharmacia) before AcLDL and 7KAcLDL were incubated with cells. The LDL preparations were stored at 4 °C, under N_2, in the dark and used within 7 days.

Prior to incubation with matured THP-1, AcLDL, and 7KAcLDL were enriched with ^{3}H-cholesterol. The AcLDL/7KAcLDL preparations (final LDL concentration 0.1 mg/mL) were incubated with FBS (final concentration 1% v/v) in a tenth of the final volume of RPMI and an ethanolic solution of ^{3}H-cholesterol (final concentration 1 μCi/mL; final ethanol concentration 0.1% v/v) for 6 h or overnight at 37 °C and then diluted with RPMI to the final concentrations (*21*).

Culturing and Sterol Loading of THP-1. THP-1 monocytes were cultured in RPMI containing 10% FBS (v/v) at 37 °C in 5% CO_2 at a cell density between 0.4 and 1.2 $\times$ 10^6 cells/mL. Cells were plated in a 22-mm diameter dish at a density of 1.2 $\times$ 10^6 cells/mL in RPMI with 10% (v/v) FBS and 50 ng/mL PMA and matured into differentiated macrophages for 72 h (*21*).

Matured THP-1 cells were extensively washed with FBS-free RPMI and then incubated with the lipoprotein-containing media (total AcLDL concentration 100 μg/mL) and 50 ng/mL of PMA for 48 h. Cells were then washed again and allowed to equilibrate overnight in lipoprotein-free RPMI containing 1 mg/mL BSA and 50 ng/mL PMA. All cells were washed in FBS-free RPMI before efflux. These treatments do not influence subsequent cholesterol efflux (*21*).

Some THP-1 cells were treated with an ACAT inhibitor (5 μg/mL S-58035, Sandoz) continuously during lipoprotein loading, the equilibration period and the subsequent efflux period. The ACAT inhibitor was prepared as an ethanolic stock solution of 10 μg/mL and therefore increased the ethanol content of the respective solutions by 0.05% (v/v).

Cholesterol Efflux. Cholesterol efflux was induced by RPMI containing 1 mg/mL BSA $\pm$ 25 μg/mL lipid-free apoA-1, 50 ng/mL PMA and $\pm$ 5 μg/mL Sandoz 58035 at 37 °C. Efflux to apoA-1 is maximal at 25 μg/mL apoA-1 (*4*, *21*). Lipid-free apoA-1 was obtained as previously described (*5*). Cholesterol efflux was determined by measurement of ^{3}H-cholesterol appearing in the media with the start of apoA-1 incubation as time zero. For that purpose, 100 μL aliquots of the efflux media were taken at various times and spun in Eppendorf tubes at 800*g* to remove loose cells. A total of 80 μL of supernatant was transferred to scintillation vials and counted. At the end of the time course, the media were removed, the cells washed in ice-cold PBS and lysed in 1 mL of NaOH (0.2 M). A fraction (100 μL) was counted to calculate the counts in the cell portion of the culture. The efflux (unless otherwise stated) is expressed as a percentage of the total counts (media + cells).

Cellular Sterol Analysis. Supernatants of the efflux media and cell lysed were extracted as described previously (*5*). Cholesterol, 7K, and their respective esters were analyzed by reverse-phase HPLC (*22*, *23*).

Protein Determination. LDL and cell protein was determined by the bicinchoninic acid assay method using BSA as a standard (*5*).

Mathematical Modeling. A number of kinetic models describing cholesterol efflux from cells have been established and evaluated against the experimental data. For all models first-order kinetic equations have been assumed:

$$\frac{dE}{dt} = \sum_i [k_i \times c_i] \qquad (1)$$

where E is the cholesterol efflux, k_i rate constant, and c_i the unesterified and esterified cholesterol concentration from

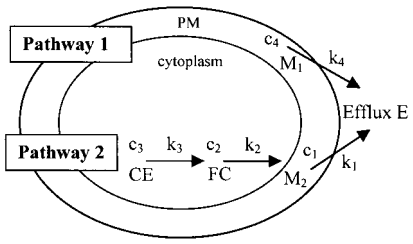

FIGURE 1: Schematic representation of proposed mathematical model. The rate constants, $k_1 - k_4$, are effective rate constants. The cholesterol domains are labeled $c_1 - c_4$ and have been associated with M_2, FC, CE, and M_1, respectively, based on previous observations (*16*). M_1 and M_2 are indicating two different plasma membrane domains. FC and CE stands for free cholesterol and cholesterol esters in the cytoplasm.

cellular compartments (e.g., plasma membrane cholesterol and cytosol). The concentrations in these models are expressed in percentages of the total cholesterol in the system and the rate constants in unit time (h). The differential equations from the proposed model as schematically shown in Figure 1 are as follows:

$$\frac{dE}{dt} = k_1 c_1(t) + k_4 c_4(t)$$

with

$$c_3(t) = c_3^0 e^{-k_3 t} \text{ and } c_4(t) = c_4^0 e^{-k_4 t}$$

where c_3^0 and c_4^0 are the respective cholesterol concentrations at time zero and

$$\frac{dc_1(t)}{dt} = -k_1 c_1(t) + k_2 c_2(t)$$

$$\frac{dc_2(t)}{dt} = k_3 c_3(t) - k_2 c_2(t)$$

This set of first-order linear equations can be integrated and substituted to obtain an expression of E (eq 2):

$$E = \frac{-k_1 k_2 c_3^0}{(k_2 - k_3)(k_1 - k_3)} \exp(-k_3 t) - \frac{A_1 k_1}{(k_1 - k_2)} \exp(-k_2 t) - A_2 \exp(-k_1 t) - c_4^0 \exp(-k_4 t) + A_3$$

A_1, A_2, and A_3 are integration constants. The boundary conditions are such that the efflux $E = 0$ at time zero, which allows the determination of A_3. c_2, c_1, and c_3 are greater than zero for all t which limits the choice of A_1 and A_2.

If reverse rate constants are incorporated into the model there is no longer an analytical solution. To solve such a model a Runge−Kutta algorithm was used to obtain an expression for E. The calculated values for the efflux E over time was then fitted to the experimental data using a nonlinear least-squares curve fitting program (Microsoft Excel 2000). The fitting of the theoretical expression to the data was evaluated using normalized squares of the residuals as an error function, ERF:

$$\text{ERF} = \frac{1}{\sum_i y_{\text{obs}}^2(\text{i})} \times \sum_i [y_{\text{obs}}(\text{i}) - y_{\text{calc}}(\text{i})]^2 \qquad (3)$$

where y_{obs} and y_{calc} are the experimental and theoretical values for the cholesterol efflux, respectively. Although each data point counts as equal weight in this error function, differences between data and theory for greater y's will dominate the error function; this error function is therefore suitable (and widely used) where the systematic error for small values is larger than for greater values. A fit is regarded as unsuitable for the experimental data when 1 > ERF > 0.1, reasonable when 0.1 > ERF > 0.01 and excellent when 0.01 > ERF > 0.001.

While the error function describes the overall quality of the fit it does not provide any statistical evaluation of the established regression coefficient (in this case the rate constants). The standard deviation of the regression coefficient k_i is given by (*24*)

$$\sigma_i = \sqrt{P_{ii}^{-1}}\, \text{SE(y)} \qquad (4)$$

where $\mathbf{P}_{ii}^{-1}$ is the ith diagonal element of the inverse of the $\mathbf{P}_{ij}$ matrix,

$$P_{ij} = \sum_{n=1}^{N} \frac{\delta E_n}{\delta k_i} \frac{\delta E_n}{\delta k_j}$$

with $\delta E_n/\delta k_i$ the partial derivative of the efflux function with respect to k_i evaluated at the time point t_n and

$$\text{SE(y)} = \sqrt{\frac{\sum (y_{\text{obs}} - y_{\text{calc}})^2}{N - K}}$$

and N the number of data points and K the number of regression coefficients to be determined. The differential terms $\delta E_n/\delta k_i$ can be calculated for each data point by numerical differentiation. The term k_i is varied by a small amount from its optimized value while the others k_j terms are held constant. This process is repeated for each of the K regression factors, then the cross product $(\delta E_n/\delta k_i)(\delta E_n/\delta k_j)$ for each of the N data points is obtained and the sum $\sum(\delta E_n/\delta k_i)(\delta E_n/\delta k_j)$ is computed. That allows the construction of the terms of the $\mathbf{P}_{ij}$ matrix which is then inverted and the terms along the main diagonal of the inverse matrix are then used to calculate the standard deviations of the coefficients using eq 4.

RESULTS

Sterol Loading of and Efflux from THP-1 Macrophages. As previously shown, model foam cells can be created in vitro by exposing mature macrophages to acetylated LDL (AcLDL) for 48 h which leads to an increased cholesterol content (~92 nmol sterol/mg of cell protein versus ~21 nmol/mg for nonloaded cells) of which between 30 and 60% (mean 46%) is esterified (see Table 1). By changing the ratio of 7KAcLDL to AcLDL in the loading media from 0:1 to 1:3 macrophages can be both cholesterol loaded and selectively and progressively enriched with 7K. The percentage of the 7K in terms of total sterol content can be increased from 0 to 20% without inducing cell death, as measured by lactate dehydrogenase release and cell protein content.

Uptake of lipoprotein enriched with ^{3}H-labeled cholesterol allows rapid analysis of subsequent cholesterol efflux. Efflux to apoA-1 (25 μg/mL) was started after an overnight

Table 1: Sterol Content of THP-1 Macrophages after 24 h Incubation with AcLDL ± 7KAcLDL and ± an ACAT Inhibitor[a]

loading conditions (μg of LDL protein/mL)						
AcLDL	7KAcLDL	FC (nmol/mg)	CE (nmol/mg)	7K (nmol/mg)	7KE (nmol/mg)	7K (%)
100	0	63.21 (6.64)	28.69 (5.19)	n.d.	n.d.	0
95	5	57.49 (5.04)	40.55 (6.85)	3.42 (0.42)	0.189 (0.06)	3.55
90	10	46.72 (3.28)	69.37 (15.61)	6.74 (0.74)	8.97 (1.82)	11.91
85	15	55.74 (5.03)	45.61 (10.31)	9.10 (1.39)	8.53 (3.19)	14.82
80	20	62.23 (5.47)	61.54 (15.57)	12.55 (1.17)	14.52 (1.72)	17.95
75	25	52.76 (6.54)	63.02 (7.63)	12.53 (1.48)	18.07 (4.32)	20.91
+ S-58035						
100	0	80.64 (7.09)	<1	n.d	n.d.	0
95	5	79.79 (9.89)	<1	4.26 (0.40)	n.d.	5.07
90	10	95.13 (8.59)	<1	9.53 (1.45)	<0.01	9.11
85	15	93.86 (6.60)	<1	14.37 (1.69)	<0.01	13.28
80	20	90.88 (9.54)	<1	17.63 (1.95)	<0.02	16.25
75	25	88.92 (7.80)	<1	22.28 (2.74)	<0.02	20.04

[a] 1.2×10^6 cells were incubated with a total of 0.1 mg/mL AcLDL/7KAcLDL and the ratio of AcLDL to 7KAcLDL was varied. For loading conditions and sterol analysis, see methods. All sterols are given in nmol/mg cell protein and are means of triplicate cell cultures. Standard deviations are given in brackets. The percentage of 7K content is 100 × (F7K + 7KE)/(CH + CE + F7K + 7KE). F7K stands for unesterified 7K, 7KE for 7K esters, CH for unesterified cholesterol and CE for cholesterol esters.

equilibration period to allow the metabolism of the endocytosed cholesterol. Taking the loading and equilibration period together, efflux was initiated 65 h after initiation of PMA-induced differentiation. It was assumed that any effects of PMA on the activity of second messenger systems and expression of membrane proteins such as SR-B1 or ABCA1 had reached a stable level by this time. PMA was previously shown to have no effect on SR-B1 expression in THP-1 cells over this time scale (*25*). Efflux is always expressed as the percentage of total radioactivity in the cell culture released into the media. Kritharides et al. have shown that under the conditions used here the ^{3}H-cholesterol efflux is representative of cholesterol mass efflux (*4*). Furthermore, the presence of 50 ng/mL PMA during the efflux period does not affect cholesterol export to apoA-1 (*21*). Figure 2a shows a typical cholesterol efflux experiment from 0 to 3 h from AcLDL-loaded cells. Cholesterol efflux to 1 mg/mL BSA is minimal after approximately 30 min and to protein-free RPMI >1% during the entire efflux period. The apoA-1-induced efflux from cholesterol-loaded cells can be qualitatively split into three time regions; the initial efflux from 0 to 0.75 h, a "lag phase" from 0.75 to 1.5 h and the beginning of a second efflux period (> 1.5 h). The same triphasic shape was observed for cholesterol efflux from cells supplemented with 7K (Figure 2b), although the magnitude of efflux was increasingly depressed in the presence of increasing concentration of 7K.

Mathematical Modeling for Cholesterol Efflux Data. We sought to find the simplest mathematical model which would describe the data shown in Figure 2a (efflux from cholesterol-loaded cells), to establish the rate constants which describe the cholesterol efflux and compare them in different experimental conditions. The model started as the simplest possible (see *E*(calc1) below) and was extended stepwise to more complex versions. This systematic approach was chosen to rule out a number of cholesterol efflux mechanisms where their corresponding data from the models did not describe the experimental data. Additional caution has to be taken with over-complex models: by introducing more than the necessary number of rate constants and cholesterol domains or sources, the degree of freedom given to the fitting algorithm increases. This in turn decreases the accuracy of the fit and makes a comparison of the rate constant for different experiments meaningless. Although a simpler mathematical model may not fully describe all possible cholesterol movement, it describes those which are rate limiting and relevant for the time period which was investigated.

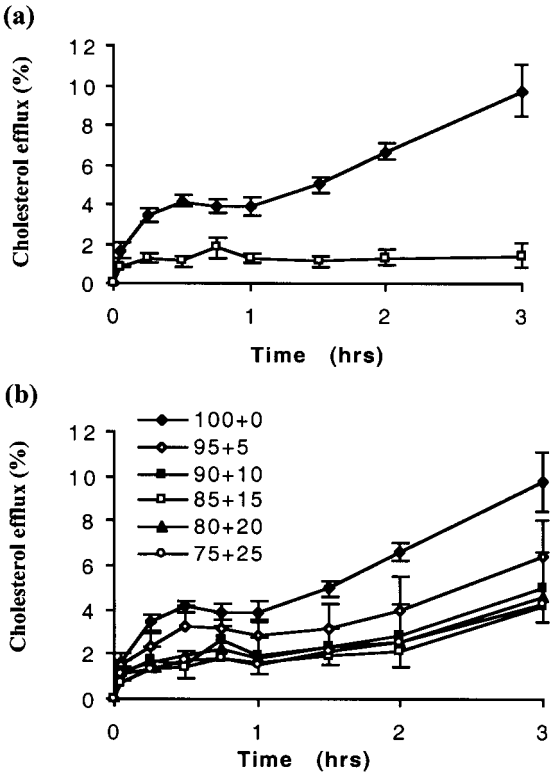

FIGURE 2: Cholesterol efflux over the first 3 h to 1 mg/mL BSA in RPMI with (◆) or without (□) 25 μg/mL apoA-1 from AcLDL-loaded cells (a) and to apoA-1 (25 μg/mL) from AcLDL/7KAcLDL-loaded cells (b). AcLDL/7KAcLDL ratios of the loading conditions for (b) are given in the legend (100 μg/mL total lipoprotein concentration). Efflux is given as percentage of total cholesterol in the cell culture and has been averaged over three experiments. The error bars represent the standard deviations.

(A) Previously Described Models. Over 12 models have been evaluated and three of those are shown in Figure 3. The first (model 1, Figure 3) is the simplest possible, consisting of a single cholesterol "source" with a single rate constant. This model has the classical equation for desorption,

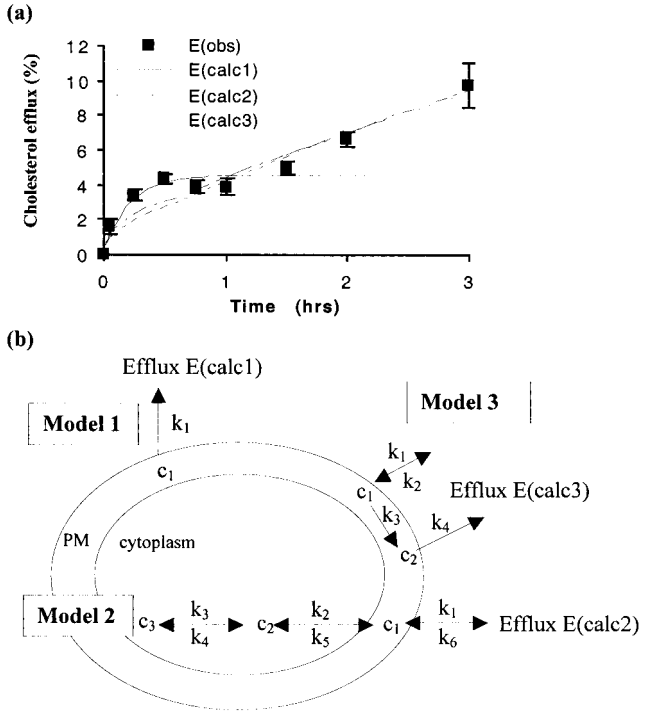

FIGURE 3: (a) Experimental cholesterol efflux, *E*(obs), from AcLDL-loaded cells to 25 μg/mL apoA-1 (see Figure 1) and three mathematical models which have been ruled out. Panel b illustrates the three models. The first model, *E*(calc1), is the simplest model possible and treats the cell as one cholesterol pool (c_1) and efflux $E(t) = E_{max} - E_{max} \times \exp(-kt)$ with $E_{max} = 4.5$ and $k = 4.6$. The second model, *E*(calc2) has been proposed by Morel et al. and describes the bidirectional cholesterol flux from "cholesterol esters" (source, c_3) to free intracellular cholesterol (intermediate 1, c_2) to plasma membrane cholesterol (intermediate 2, c_1) to the media (product, *E*). The third model, *E*(calc3), has been previously published by Kritharides et al. and an inter-linked "slow pool" (source 1, c_1) and "fast pool" (source 2, c_2) which both contribute to the efflux. Models 2 and 3 have no analytical solution and were solved with a Runge−Kutta algorithm as described in methods. All three models have a poor fit as reflected in the high value of the error function; ERF = 0.147, ERF = 0.031, ERF = 0.031 for model 1, 2, and 3, respectively.

$E = c_0 - c_0 e^{-k_1 t}$, and it can describe the cholesterol efflux from liposomes to apoA-1 (data not shown). However, Figure 3a and an error function ERF > 0.1 highlights the unsuitability of that model for cellular efflux − *E*(calc1, ERF = 0.147).

This model was extended step-by-step by incorporating consecutive first-order reactions with one "source", a final "product" (the cholesterol in the media) and 1−3 "intermediates". Additionally, reverse rate constants were also introduced. These consecutive models (varying only in their number of intermediates and reverse rate constants) could only adequately describe the "second" efflux period (>1.5 h) or part of the initial efflux but not the lag phase seen between 0.75 and 1.5 h. Figure 3 (see model 2, Figure 3, *E*(calc2) ERF = 0.03051) shows the calculated efflux from such a consecutive model with 1 source, 2 intermediates, a final product and 6 rate constants. This particular model has been proposed by Morel et al for efflux to HDL and albumin (*19*) and fits reasonably for efflux to delipidated apoA-1 with an ERF of 0.03.

Apart from introducing intermediate steps, the model can be expanded by assuming that the cholesterol exported is derived from more than one source and/or via more than one pathway. A "two pool model" (model 3, Figure 3b) has been proposed for efflux to lipidated acceptors over a 24 h period which can be interpreted as two connected parallel pathways which both contribute to the efflux (although their data could also be fitted to a consecutive model) (*10*, *20*). However, this model does not fit our data for efflux to apoA-1 any better over the first 3 h than the "single source" model outlined above (Figure 3, *E*(calc3), ERF = 0.030825).

(B) Proposed Model. The new model proposed consisting of two pathways is shown in the scheme in Figure 1. The first pathway (pathway 1) represents the efflux of cholesterol from a plasma membrane domain directly to apoA-1. The second pathway (pathway 2) exists in parallel with pathway 1. Pathway 2 is the conventional consecutive pathway in which intracellular cholesterol esters are hydrolyzed to cholesterol in the cytoplasm followed by transport into the plasma membrane and then release to apoA-1. All rate constants are effective rate constants assuming that reverse cholesterol flux is minimal at early time points. This model provides an excellent fit to the experimental data as illustrated for AcLDL-loaded cells in Figure 4a and b. The rate constants used to obtain this fit for the AcLDL-loaded cells are summarized in Table 2. The only deviation from the data is at 24 h. However, at this time point, additional mechanisms may be occurring, such as cholesterol synthesis and cholesterol influx, which are not incorporated into the model. Hence, the proposed new model only seeks to explain the unexpected efflux behavior in the first 3 h (0−3 h). Once the theory has been fitted to the experimental data the model defined by eq 2 allows the calculation of the exported cholesterol from the various cholesterol-containing compartments (Figure 4c). These four compartments c_1 to c_4 are as illustrated in Figure 1.

Let us look at the proposed model in more detail. The two parallel pathways pose three key issues. First, the time period over which each pathway is significant must be addressed. Second, a link between the two pathways for cholesterol efflux is considered. Finally, what are the initial concentrations of cholesterol in each of the domains in Figure 1 (see boundary conditions).

Turning to the time period for each pathway: pathway 1 describes the fast initial efflux while pathway 2 is dominant at time periods greater than 1.5 h. To keep the model as simple as possible, the number of required "intermediates" should be kept to a minimum. Pathway 1 does not require any intermediates at all and hence has only a "source" (M_1 in Figure 1). Since the pathway 2 possesses a "lag phase", intermediates need to be postulated. M_2 as shown in Figure 1 is one intermediate and by introducing a second one, FC, the fit improves from ERF = 0.022902 (just with M_2) to ERF = 0.002348 (FC and M_2). The fitting however is not significantly improved (<2%) by introducing reverse rate constants. Since only cholesterol efflux for the first 3 h was investigated (with the amount of extracelluar cholesterol being low and the direction of cholesterol flux obvious) the model was not further complicated by including reverse rate constants.

Linking the two pathways can be achieved mathematically simply by including a rate expression for cholesterol exchange between M_2 and M_1. Linking M_2 and M_1, however, provides minimal improvement in the error function of the

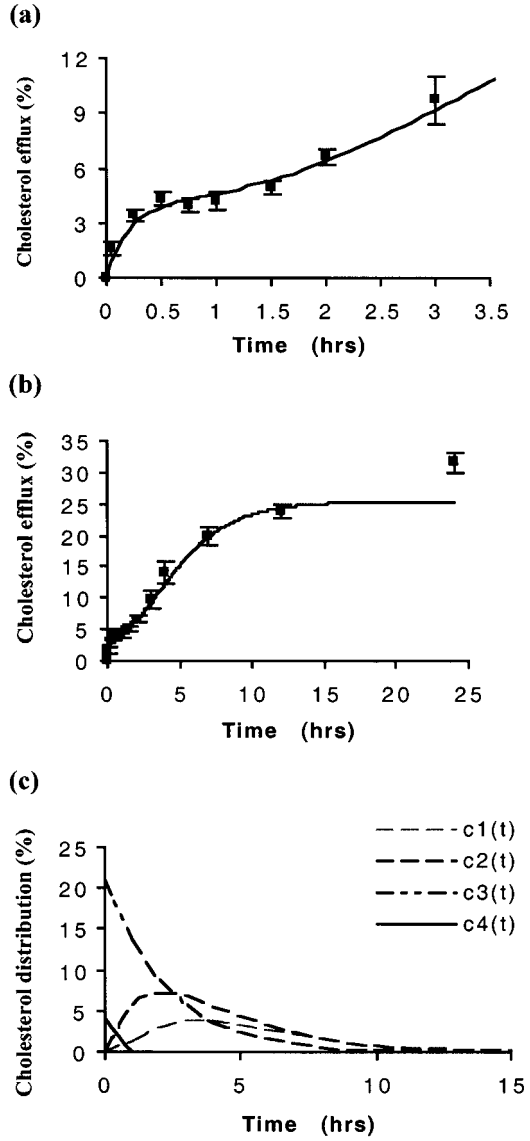

FIGURE 4: Cholesterol efflux data from AcLDL loaded cells (■) (see also Figure 2) and the calculated efflux (—) from the proposed model outlined in Figure 1. The analytical solution for the model is given in methods. (a) is an enlargement of the early time period of (b), and (c) shows the cholesterol distribution as calculated from the model. The error function of the fit is ERF = 0.002348 for data points from 0 to 12 h and the rate constants are given in Table 2.

fit. The values of the rate constants for this link are small relative to the rate constants for the efflux showing that if such a link exists it does not significantly influence the rate of efflux. From the perspective of the model, introducing this linking mechanism compromises the robustness of the model; allowing more than one realistic fitting solution. The absence of a link between M2 and M1 implies that the source M1 does not get "refilled" (see Figure 4c) and that the first pathway does not contribute to the cholesterol efflux after 1 h. Hence, it is important to note that a link between the two pathways has no significant effect on theoretically described cholesterol efflux; however, its absence does not preclude the possible existence of a physical exchange of cholesterol between the two plasma membrane domains.

The final issues to be addressed are the initial values of c_1, c_2, c_3, and c_4 used to obtain the fit between theory and experiment. The starting value (or time zero source size) for c_4 is derived by the algorithm from the amount of exported cholesterol at 1 h. The starting value for the other intermediates were set to zero, and hence all cholesterol at time zero is either stored as cholesterol esters (c_3) or M1 (c_4). This is consistent with cells storing the majority of the excess cholesterol as cholesterol esters in the cytoplasm and as free cholesterol in the plasma membrane. Fortuitously, in the computer aided fitting the algorithm chose values of zero for c_2 and c_1 at time zero.

Experimental Support for the Proposed Model: Role of Ester Hydrolysis during Cholesterol Efflux. The discussion above highlights the excellent agreement between the new model and the experimental data and enables the values of rate constants to be derived. However, the question still exists as to whether the theoretically determined rate constants are valid. Such a question can only be answered with independent experimental assessment of the rate constants. In the case of k_3 such assessment should be possible by either using an inhibitor to remove the ester hydrolysis step or independently determining the rate of that particular step in the pathway.

Incubating mature macrophages with an ACAT inhibitor (S-58035) during the LDL uptake suppresses sterol esterification and produces a large intracellular free cholesterol content (see Table 1). Figure 5a shows the early cholesterol efflux from cells treated with ACAT inhibitor. Prevention of esterification increases cholesterol efflux to apoA-1 mainly

Table 2: Rate Constants and Cholesterol "Pools" for Efflux from AcLDL and 7K-AcLDL Loaded Cells as Described by the Mathematical Model Schematically Shown in Figure 1[a]

cell loading conditions (μg of LDL protein/mL)								
AcLDL	7KAcLDL	k_1 (h^{-1})	k_2 (h^{-1})	k_3 (h^{-1})	k_4 (h^{-1})	c_3^0(%)	c_4^0(%)	ERF × 10^{-3} (%)
100	0	0.791 (0.001)	0.494 (<10^{-4})	0.428 (<10^{-4})	4.611 (1.004)	21.099 (0.026)	4.241 (0.196)	2.3
95	5	0.548 (0.001)	0.345 (<10^{-4})	0.294 (<10^{-4})	4.815 (1.256)	21.795 (0.034)	3.465 (0.188)	3.5
90	10	0.518 (0.001)	0.322 (<10^{-4})	0.277 (<10^{-4})	4.726 (1.669)	21.891 (0.035)	2.526 (0.187)	1.1
85	15	0.485 (<10^{-3})	0.302 (<10^{-4})	0.259 (<10^{-4})	4.665 (1.485)	21.918 (0.025)	1.915 (0.128)	4.2
80	20	0.458 (0.001)	0.301 (<10^{-4})	0.259 (<10^{-4})	4.666 (1.919)	21.918 (0.033)	1.911 (0.166)	8.1
75	25	0.458 (0.001)	0.301 (<10^{-4})	0.259 (<10^{-4})	4.666 (1.455)	21.918 (0.025)	1.911 (0.126)	14.1
+ S-58035 100	0	1.318 (0.003)	0.740 (<10^{-3})	0.549 (<10^{-3})	11.691 (4.992)	30.401 (0.058)	3.912 (0.244)	3.1

[a] c_3 can the associated with intracellular esterified cholesterol (as shown in Figure 1) or with an intracellular free cholesterol storage "pool" for S-58035 treated cells. c_3^0 and c_4^0 are the cholesterol concentrations at time zero for c_3 and c_4, respectively. c_1^0 and c_2^0 are zero at time zero for all conditions. All rate constants are given in h^{-1} and their standard deviation is given in brackets. ERF gives the quality of the overall fit as outlined in methods.

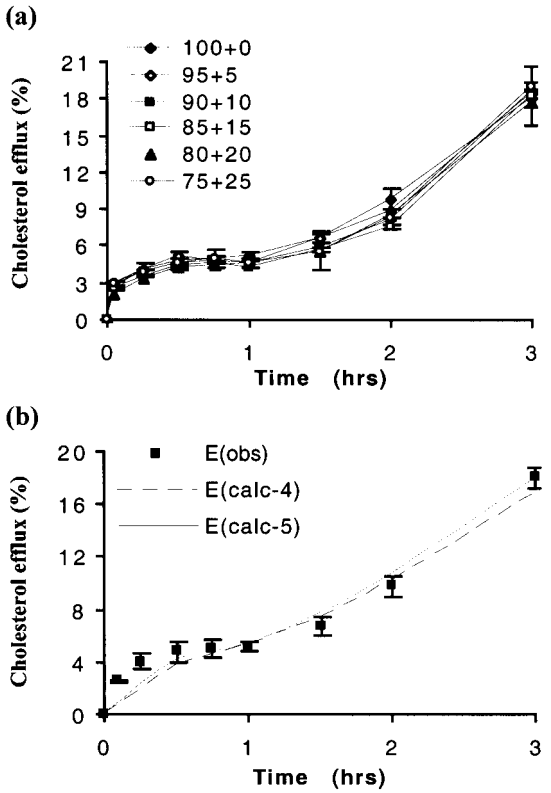

FIGURE 5: Cholesterol efflux to apoA-1 (25 μg/mL) from cells treated with an ACAT inhibitor (S-58035, 5 μg/mL) during the loading, equilibration, and efflux period. For experimental details see methods and for sterol analysis of the cells see Table 1. (a) Cells have been loaded with AcLDL + 7KAcLDL as given in the legend (in μg/mL; total lipoprotein concentration 100 μg/mL). Each data point is an average of three cell cultures and the error bars represent the standard deviation. (b) The calculated efflux from two different models versus the experimental data. *E*(calc-4) assumes that $k_3 = 0$ and CE = 0 (see scheme in Figure 3), while *E*(calc-5) assumes that k_3 and CE are not equal to zero. The error function are ERF = 0.002530 and ERF = 0.003072 for *E*(calc-4) and *E*(calc-5), respectively.

via Pathway 2 since c_4^0 does not alter significantly (efflux at 1 h is similar with and without S-58035). Qualitatively, the shape of the efflux curve with S-58035 (Figure 5a) is similar to that when esters are present (Figure 2). The similarity between Figures 2 and 5a suggests that the second source (CE in Figure 1) and k_3 cannot be set to zero for the ester-free conditions. The error function of this scenario is ERF = 0.02530 (*E*(calc4) in Figure 5b), while it improves to ERF = 0.003072 (*E*(calc5) Figure 5b) when the efflux from cells without esters is fitted to the full model as shown in Figure 1. Hence, the comparison between efflux from cells with and without an intracellular ester pool suggests that k_3 is an effective rate constant describing not only ester hydrolysis but also some unknown metabolic conversion or intracellular relocation. Since k_3 increases by a factor of 1.3 by inhibiting esterification (Table 2), it can be suggested that ester hydrolysis is rate-limiting in this pathway. However, it should be noted that k_1 and k_2 also increase due to inhibited esterification (by 1.4 and 1.7, respectively) suggesting that ACAT inhibition affects not only the pathway involving esters. By "overloading" the system with unesterified cholesterol other intracellular pathways might be activated and/or additional cholesterol "pools" created, which seem to further enhance cholesterol efflux.

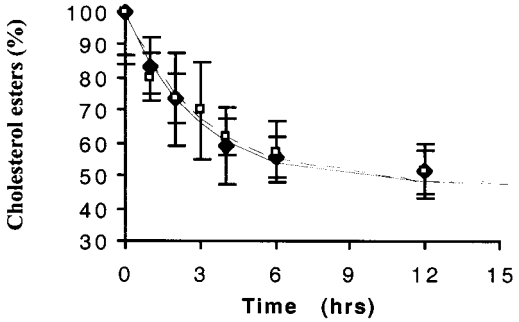

FIGURE 6: Removal of cholesterol esters over efflux time from AcLDL-loaded (◆) and AcLDL/7KAcLDL (75 μg/mL + 25 μg/mL, □)-loaded cells. Sterol esters were determined by HPLC after incubation with 25 mg/mL apoA-1 as given on the *x*-axis and expressed as sterol esters/mg cell protein. Sterol esters at time zero were then set to 100% and the other data points correlated accordingly. Incubation with 1 mg/mL BSA instead of apoA-1 removes only (7 ± 4)% of the sterol esters over a 24-h period. Each data point represents the average of three cell cultures and the error bars show the standard deviations. The solid and dashed line are empirical lines of best fit for AcLDL and AcLDL/7KAcLDL-loaded cells, respectively, using the equation $CE = CE_{max} \times \exp(-k_3 t) + (100 - CE_{max})$. CE_{max} refers to the maximum loss in cholesterol ester.

An alternative to modifying the system with an inhibitor is to directly determine the decrease in mass of cholesterol esters in the cells at various time points during efflux. Ester hydrolysis during efflux has been previously determined, and it is generally agreed that esterification of free cholesterol during efflux is not significant (*21*, *26*). Furthermore, the study by Graham et al. suggests that hydrolysis of sterol ester is the rate-limiting step in cholesterol efflux from THP-1s (*26*).

Figure 6 shows the decrease in sterol esters from cholesterol- and (cholesterol + 7K, 75+25)-loaded cells with cholesterol esters normalized to the amount of esters found at time zero. The solid line in Figure 6 is an empirical line of best fit with the equation $CE = 100 - CE_{max} + CE_{max}e^{-k_3 t}$. CE_{max} refers to the maximum loss in cholesterol esters of 51.5 ± 5 (%). This partial reduction in cholesterol esters is high compared to previously published figures (37 ± 4%; *21*, *26*); however, in both publications the esters are compared to a control experiment which was also incubated for 24 h (rather than to the start of the incubation as in this case). In preliminary experiments, we noticed that cholesterol ester loss can vary greatly in the control incubation and such variation could account for the difference in ester hydrolysis rate.

The depletion of cholesterol esters with time as plotted in Figure 6 can be used to experimentally determine the value of k_3. The experimentally determined value of rate constant $k_3 = (0.38 \pm 0.05)\ h^{-1}$ is close to the theoretically determined value of $k_{3,calc} = 0.43$. The coincidence of these two values provides an excellent indication that the model provides a realistic description of experimental system. It also supports that cholesterol ester hydrolysis is the rate-limiting step ($k_{1,2} > k_3$) in pathway 2 as proposed by Graham et al. (*26*). The data in Figure 6 also suggest that the decrease in esters is only marginally influenced by the presence of 7K with the value for k_3 only slightly smaller, $k_{3,7K} = 0.32 \pm 0.04$.

Effect of 7-Ketocholesterol (7K) on the Rate Constants for Cholesterol Efflux. 7-ketocholesterol, an inhibitor of

cellular cholesterol efflux to apoA-1, was incorporated into the sterol-loaded cells and the effect of 7K on the rate constants describing the cholesterol efflux investigated. 7K enrichment resulted in cells whose sterol content contained up to 20% 7K or 7K esters (Table 1). Furthermore, cellular subfractionation experiments (data not shown) showed that the 7K/cholesterol ratio in the cell lysate mirrored that in the plasma membrane fraction.

The cholesterol efflux data from 7K-containing cells was fitted to the scheme shown in Figure 1 and the rate constants are summarized in Table 2. c_1 and c_2 (FC and M_2) were calculated as zero at time zero for all conditions. Rate constants obtained from data for cells loaded only with free sterols (S-58035 treated cells) are not affected by increasing the 7K content (see Figure 5a), and so only rate constants from free cholesterol-loaded cells (AcLDL-loaded + S-58035) are shown in Table 2. Additionally, c_3 is not altered by 7K loading but the calculated size of the "cholesterol storage pool" c_3 differs for cells treated (30.4%) or not treated (20.9%) with S-58035.

From Table 2, it also appears that the rate constant k_4 describing cholesterol removal from M_1 is not affected by cellular 7K content. However, M1 (c_4^0) itself decreases so that the efflux from this short, initial pathway decreases by 45%. In contrast to the "fast" pathway, the rate constants of the slower pathway are affected by 7K incorporation but the cholesterol distribution remains the same. In fact, all rate constants (k_1, k_2, k_3) in that pathway decrease by 61%. Therefore k_3 also decreases to $k_{3,calc} = 0.259$. The reduction in k_3 predicted by the model is significantly greater than experimentally determined by Figure 6 ($k_{exp} = 0.32 \pm 0.04$).

Characterization of the Cholesterol Efflux Pathways. The mathematical model indicates two independent pathways by which cellular cholesterol can be exported. In the description of the model above, it was pointed out that the two pathways are operating over distinct time periods and that pathway 2 sets in after efflux via pathway 1 is completed. Hence, it is feasible that the consecutive nature of the two pathway model is not only a result of different kinetics but that pathway 1 is activating pathway 2. Such an activation step could be either intra- or extracellular. An extracellular stimulus could be partial lipidation or other modification of the lipid-poor apoA-1. If so, pathway 1 would describe the initial lipidation (or other modification) of apoA-1 and the pathway 2 the efflux to partially lipidated apoA-1.

To test this hypothesis of an extra-cellular activation of pathway 2, delipidated apoA-1 was preconditioned by exposing it to cholesterol-loaded cells for 1 h. During this incubation, pathway 1 and any possible essential modification of apoA-1 (such as partial lipidation) would be completed. The preconditioned apoA-1 was then exposed to a fresh set of cholesterol-loaded cells. If the hypothesis is correct and pathway 2 is describing cholesterol efflux to modified (e.g., partially lipidated) apoA-1 then pathway 1 (stimulated by the excess of still unmodified apoA-1) and pathway 2 (activated by the modified apoA-1) would occur simultaneously and immediately, without the usual lag-phase. Cholesterol efflux from the second set of cells is shown in Figure 7 for various cholesterol-loading conditions. It should be pointed out the cells used for apoA-1 preconditioning were sterol-loaded under the same conditions as cells used for the

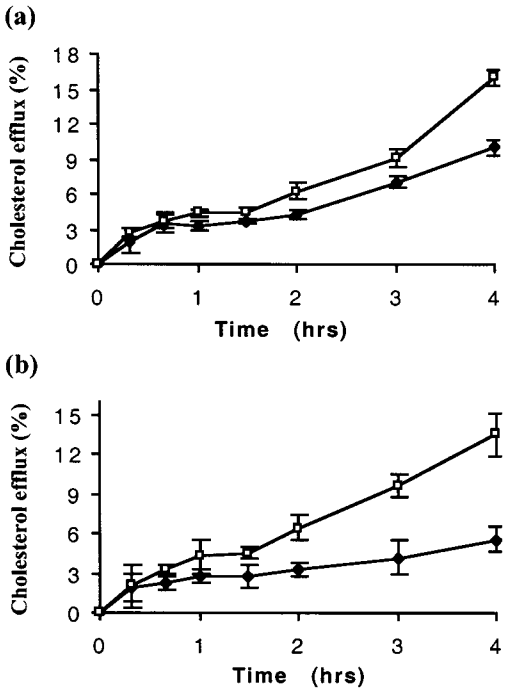

FIGURE 7: Cholesterol efflux to preconditioned apoA-1 (25 μg/mL) from (a) AcLDL-loaded cells (100 μg/mL) in the presence (□) and absence (◆) of an ACAT inhibitor (S-58035, 5 μg/mL). (b) Cells were loaded with 75 μg/mL AcLDL and 25 μg/mL 7KAcLDL in the presence (□) and absence (◆) of an ACAT inhibitor (S-58035, 5 μg/mL). Preconditioning was carried out by exposing the efflux media to lipid-loaded cells (with identical loading conditions as the efflux shown) for 1 h at 37 °C. Cells treated with an ACAT inhibitor were exposed to the inhibitor (5 μg/mL) during loading, equilibration, and efflux. The data are averages of three cell cultures and the error bars represent the standard deviation.

efflux in Figure 7. It can be seen that the kinetics of cholesterol efflux to preconditioned efflux media resemble the efflux to lipid-poor apoA-1 (shown in Figures 2 and 5a) for all loading conditions. A similar pattern of efflux from cells treated with an ACAT inhibitor was found, although the proportion of cholesterol released to preconditioned media was less than to nondelipidated apoA-1. However, the delay between pathway 1 and pathway 2 still occurs in the cholesterol efflux to preconditioned apoA-1 suggesting that the two pathways do not occur simultaneously under these conditions. Therefore, it can be concluded that pathway 2 is independent of prior modification (such as partial lipidation) of apoA-1 and may also require a intracellular trigger.

Since both pathways are stimulated by apoA-1 and the two rate constants (k_1 and k_4) are significantly different, it can be further concluded that apoA-1 can interact with at least two different sites or functional pools on the cell surface. In the scheme in Figure 1, these two "sites" are labeled M_1 and M_2. The initial values for M_1 and M_2 suggest that their cholesterol concentrations at equilibrium (in the absence of cholesterol efflux) are different. According to the model, no excess cholesterol is stored in M_2, but this domain allows apoA-1 to access intracellular cholesterol. In the site M_1, a small proportion of the excess cholesterol is stored but the site does not contribute to cholesterol efflux at later stages since the model suggests that M_1 is not replenished during efflux.

We therefore addressed whether M_1 regenerates in the absence of apoA-1. For this, sterol-loaded cells were exposed to apoA-1 for 1 h (i.e., effluxed until efflux via pathway 1 had been completed and M_1 depleted, efflux period 1); the cells were then incubated with apoA-1-free media for various lengths of time (equilibration period) before the cells were exposed to fresh apoA-1-containing media (efflux period 2). Figure 8 a and b shows the efflux periods 1 and 2 (but not the equilibration period between the two periods). The arrow indicates at which stage the efflux has been interrupted.

In Figure 8a, the efflux from AcLDL-loaded cells was interrupted at 1 h for a brief wash or for a 15 min, 30 min, or 3.5 h incubation in apoA-1-free media. By simply washing the cells with apoA-1-free media, the efflux was disturbed but the pattern of the second efflux period did suggest that M_1 was re-formed. However, if the equilibration period was prolonged, M_1 appears to be replenished, since the second efflux period shows again the fast initial efflux followed by the lag phase. A similar observation can be made for cells loaded under different conditions (AcLDL versus 7KAcLDL loading, ± an ACAT inhibitor, Figure 8b) suggesting that the site M1 becomes cholesterol rich when excess cholesterol is available for efflux but delipidated apoA-1 rapidly removes cholesterol from this site.

Since M_1 can be replenished in the absence of apoA-1, it can be investigated whether efflux from both pathways can occur simultaneously despite their different kinetics. Simultaneous efflux via the two pathways would highlight the independence of the pathways. In Figure 8c, pathway 2 was stimulated by a prolonged initial efflux period (3 h), the site M1 was replenished by a subsequent 15 min incubation with apoA-1-free media, followed by the recording of the second efflux period. As above, Figure 8c only shows the initial, 3-h efflux period and the second efflux but not the 15 min equilibration. Simultaneous efflux would be characterized by the absence of a lag-phase in the second efflux period. Figure 8c clearly shows the lag phase has persisted and therefore independence of the two pathways could not be proven. Thus, one can only speculate on reasons why the efflux pattern is so persistent with the two pathways occurring after each other. One possibility is that efflux from pathway 1 is the intracellular stimulus for pathway 2.

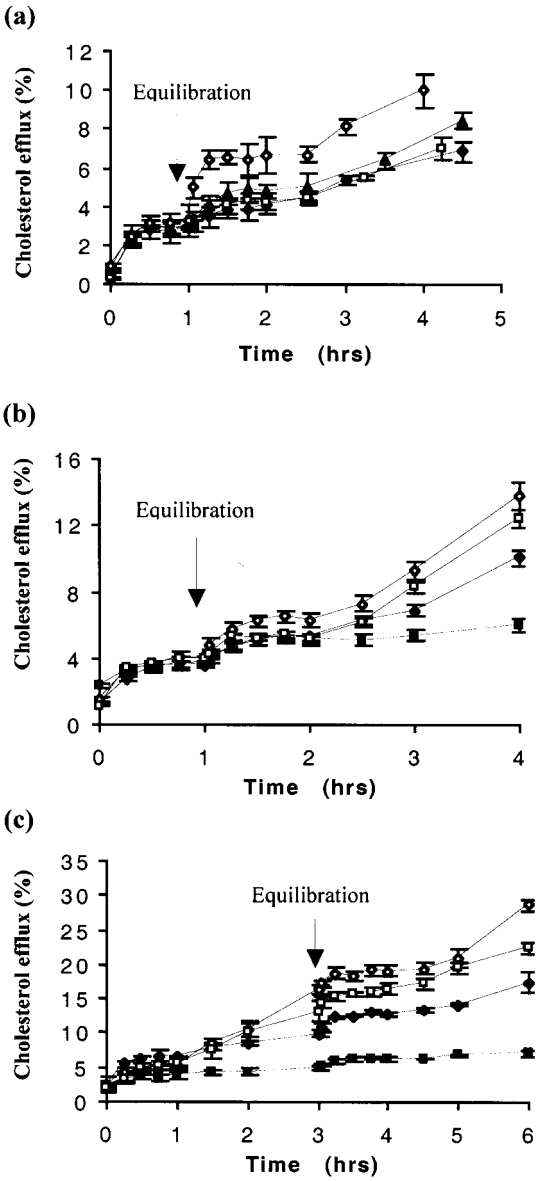

FIGURE 8: The cholesterol efflux to two sets of apoA-1-containing RPMI (25 μg/mL). After an initial efflux to apoA-1 (efflux period 1), the cells were washed three time with 1 mg/mL BSA in RPMI and then incubated with 1 mg/mL BSA in RPMI for various lengths of time (equilibration period). Cholesterol efflux was then recommenced with fresh, lipid-poor apoA-1 media (25 μg/mL). Only the two efflux periods but not the equilibration period is shown; the arrow indicates when the efflux has been interrupted. (a) Efflux from AcLDL-loaded cells (100 μg/mL) with a first efflux period of 1 h. The length of the equilibration period varied from either wash alone (◆), or followed by BSA incubation for 15 min (□), 30 min (▲) or 3.5 h (◇) (b) Efflux from cells which were loaded with 100 μg/mL AcLDL (◆) and additionally with an ACAT inhibitor (◇, S-58035 5 μg/mL) or with 75 μg/mL AcLDL + 25 μg/mL 7KAcLDL (■) and an ACAT inhibitor (□, S-58035 5 μg/mL). The first efflux period and the equilibration period were 1 h. (c) Cells were loaded as in (b). The first efflux period lasted 3 h and the equilibration period lasted only 15 min. For all three plots, the symbols and the error bars represent an average of three cell cultures and the standard deviation, respectively.

DISCUSSION

Kinetic modeling can give an insight into a dynamic system without having to interrupt or disturb it at various time points. It is therefore a very powerful tool and has been previously applied to cellular cholesterol efflux (*9*). Cholesterol efflux to cyclodextrins, for example, has been found to involve at least two kinetically distinct cholesterol pools and the different pools have been associated with different sections of the plasma membrane (*27*). Kinetic observations have also been made on efflux to different cholesterol acceptor-like HDL particles, phospholipid particles, and various apolipoproteins (reviewed (*9*)). Most cholesterol acceptors do not reveal a simple kinetic behavior and a mathematical approach can be fruitful for such systems. Morel et al applied a kinetic model for cholesterol efflux to investigate the intracellular metabolism of 25-hydroxylcholesterol (*19*). Their mathematical model comprises essentially the second pathway of the model introduced here (Figure 1), with both forward and backward rate constants. A linked parallel pathway rather than a consecutive model was assumed by the same group to describe cholesterol movement in the presence of an ACAT inhibitor. In both publications the models describe the experimental data; however, these models are not conclusive, since simpler models may also

fit the data and they have been found to be unsuitable for the data presented here.

In this paper, we evaluate a model comprising a combination of the two: a consecutive pathway comprising of a cholesterol ester storage pool, and an intracellular intermediate followed by a plasma membrane pool and a second, parallel pathway which consists only of a plasma membrane pool. This more complicated model is the simplest model which will describe the entire experimental efflux profile observed between 0 and 3 h, hence providing strong evidence of more than one pathway for cholesterol efflux. In this relatively short time period, cholesterol influx is regarded as negligible and reverse rate constants have been omitted.

The proposed model suggests that the two pathways are independent during cholesterol efflux and that cholesterol removal occurs from two different plasma membrane domains. This is highlighted by the different values for the rate constants k_1 and k_4 which both describe cholesterol removal from plasma membrane for the two pathways. Since the model only takes into account the net efflux cholesterol, basal cholesterol exchange between domains are not evaluated and may take place. Such cholesterol exchange makes an experimental verification of cholesterol distribution as calculated from the model (see Figure 4c) difficult. However, the removal of cholesterol esters during efflux can be experimentally determined and an excellent agreement between model and experiment was found. This finding strongly supports the outline of the model.

The two pathways differ greatly in their half-lives; in fact, the second, slower pathway only becomes significant after completion of the first. This leads to the hypothesis that the first process may result in activation of the second, either through an intracellular signaling pathway or through the modification of the extracellular acceptor. The latter hypothesis was excluded by preincubating the acceptor in efflux medium on sterol-loaded cells and then transferring it onto a new set of sterol-loaded cells. The initial efflux kinetic remains for the second set of cells, as does the distinct lag phase between the two pathways. If modification of apoA-1 were a trigger or requirement for the second pathway then this pathway would have been activated by the preincubated media and the lag phase would not have remained. Furthermore, this experiment suggests that M_1 and M_2 are two different plasma membrane domains for example controlled differentially by membrane proteins such as SR-B1 and ABCA1. If a direct interaction of apoA-1 with the plasma membrane is assumed, as proposed by the microsolubilization theory, then it would seem that apoA-1 can interact with more than one plasma membrane domain and the kinetics of the interactions are determined by the composition of the lipid domains.

By incorporating 7-ketocholesterol (7K), an oxysterol which significantly impairs cholesterol efflux, the two pathways are differently affected. The first pathway is depleted, since the size of the plasma membrane compartment M_1 decreased by more than 50% in the presence of 20% 7K while the rate constant k_4, which describes cholesterol removal from M_1, remained constant. This observation suggests that 7K is influencing the plasma membrane structure, by decreasing the size or abundance of the lipid pool which characterizes M_1. Since the functioning of such a plasma membrane domain is critically dependent on its sterol content, it might be speculated that M_1 is associated with cholesterol-rich rafts. In this case, 7K may affect the lipid raft formation, leaving only a small number of "functional" lipid rafts. However, other plasma membrane pools or other alternative explanations may apply. For example, 7K may act indirectly by affecting the expression or activity of membrane proteins implicated in cholesterol export from cells. ABCA1 appears to be essential for cholesterol export to lipid-free apolipoproteins. Nonfunctional ABCA1 is the molecular basis of Tangier disease in which HDL production and cholesterol efflux to apoA-1 are ablated or substantially depressed (*16*). ABCA1 may facilitate apoA-1 binding to the plasma membrane (*16*) and/or modulate membrane lipid distribution and availability for export (*17*, *18*), either of which may influence the fast and slow efflux pathways described. ABCA1 m-RNA expression is strongly upregulated by oxysterol ligands for LXR (e.g., 22-hydroxycholesterol) and to a much lesser degree by 7K (*28*). However, the effects of 7K on ABCA1 protein and activity remains unknown. As 7K has an inhibitory effect on cholesterol export to apoA-1, simple upregulation of ABCA1 expression is unlikely to be causal. It remains possible that this oxysterol modulates membrane lipid translocation associated with ABCA1 activity rather than ABCA1 protein itself.

In pathway 2, all rate constants are decreased by 61% by 7K while the cholesterol distribution remains. Hence, 7K does not solely affect one step in this pathway, but decreases the overall rate. If there is a signaling element involved in cholesterol removal as described by the second pathway, the decrease in all rate constants suggests that the initial signal was diminished. Since incorporation of 7K reduces the efflux of the first pathway it can be hypothesized that the initial efflux comprises the "activation signal" which subsequently affects the efflux from the second pathway. It would seem likely that such a cellular activation or signaling step involves functional membrane proteins, of which ABCA1 is the most obvious candidate at present. We have provided evidence that the "activation signal" acts at the cellular level rather than through apoA1 modification, although this does not exclude the possibility that initial apoA-1 modification (e.g., lipidation) is also required for pathway 2.

SR-B1 stimulates efflux of cholesterol to lipidated acceptors and cannot presently be excluded as a potential mediator of pathway 2. SR-B1 is present predominantly in lipid rafts in THP-1 macrophages (*25*). Consequently, any effect of 7K on lipid raft abundance and structure could impact on SR-B1 activity, and its is known that SR-B1 expression is mildly suppressed by 7K (*29*). However, further studies are clearly necessary to determine the roles of specific plasma membrane proteins and other structures in the pathways we have defined kinetically.

REFERENCES

1. Brown, A. J., Leong, S. L., Dean, R. T., and Jessup, W. (1997) *J. Lipid Res. 38*, 1730−1745.
2. Crisby, M., Nilsson, J., Kostulas, V., I., B., and Diczfalusy, U. (1997) *Biochim. Biophys. Acta 1344*, 278−285.
3. Kilsdonk, E., Morel, D., Johnson, W. J., and Rothblat, G. H. (1995) *J. Lipid Res. 36*, 505−516.
4. Kritharides, L., Jessup, W., Mander, E. L., and Dean, R. T. (1995) *Arterioscler. Thromb. Vasc. Biol. 15*, 276−289.

5. Gelissen, I. C., Brown, A. J., Mander, E. L., Kritharides, L., Dean, R. T., and Jessup, W. (1996) *J. Biol. Chem. 271*, 17852−17860.
6. Gelissen, I. C., Rye, K. A., Brown, A. J., Dean, R. T., and Jessup, W. (1999) *J. Lipid Res. 40*, 1636−1646.
7. Johnson, W. J., Mahlberg, F. H., Rothblat, G. H., and Phillips, M. C. (1991) *Biochim. Biophys. Acta 1085*, 273−298.
8. Mendez, A. J. (1997) *J. Lipid Res. 38*, 1807−1821.
9. Phillips, M. C., Johnson, W. J., and Rothblat, G. H. (1987) *Biochim. Biophys. Acta 906*, 223−276.
10. Rothblat, G. H., Mahlberg, F. H., Johnson, W. J., and Phillips, M. C. (1992) *J. Lipid Res. 33*, 1091−1097.
11. Karlin, J. B., Johnson, W. J., Benedict, C. R., Chacko, G. K., Phillips, M. C., and Rothblat, G. H. (1987) *J. Biol. Chem. 262*, 12557−12564.
12. Ji, Y., Jian, B., Wang, N., Sun, Y., Moya, M. L., Phillips, M. C., Rothblat, G. H., Swaney, J. B., and Tall, A. R. (1997) *J. Biol. Chem. 272*, 20982−20985.
13. De La Llera-Moya, M., Rothblat, G. H., Connelly, M. A., Kellner-Weibel, G., Sakr, S. W., Phillips, M. C., and Williams, D. L. (1999) *J. Lipid Res. 40*, 575−580.
14. Gillotte, K. L., Davidson, W. S., Lund-Katz, S., Rothblat, G. H., and Phillips, M. C. (1998) *J. Lipid Res. 39*, 1918−1928.
15. Gillotte, K. L., Zaiou, M., Lund-Katz, S., Anantharamaiah, G. M., Holvoet, P., Dhoest, A., Palgunachari, M. N., Segrest, J. P., Weisgraber, K. H., Rothblat, G. H., and Phillips, M. C. (1999) *J. Biol. Chem. 274*, 2021−2028.
16. Oram, J. F., and Vaughan, A. M. (2000) *Curr. Opin. Lipidol. 11*, 253−260.
17. Schmitz, G., and Kaminski, W. E. (2001) *Front. Biosci. 6*, D505−514.
18. Chambenoit, O., Hamon, Y., Marguet, D., Rigneault, H., Rosseneu, M., and Chimini, G. (2001) *J. Biol. Chem. 276*, 9955−9960.
19. Morel, D. W., Edgerton, M. E., Warner, G. E., Johnson, W. J., Phillips, M. C., and Rothblat, G. H. (1996) *J. Lipid Res. 37*, 2041−2051.
20. Mahlberg, F. H., and Rothblat, G. H. (1992) *J. Biol. Chem. 267*, 4541−4550.
21. Kritharides, L., Chistian, A., Stoudt, G., Morel, D., and Rothblat, G. H. (1998) *Arterioscler. Thromb. Vasc. Biol. 18*, 1589−1599.
22. Brown, A., Dean, R., and Jessup, W. (1996) *J. Lipid Res. 37*, 320−335.
23. Kritharides, L., Jessup, W., and Dean, R. T. (1993) *Anal. Biochem. 213*, 79−89.
24. Johnson, K. J. (1980) *Numerical Methods in Chemistry*; Marcel Dekker, New York.
25. Matveev, S., van der Westhuyzen, D. R., and Smart, E. J. (1999) *J. Lipid Res. 40*, 1647−1654.
26. Graham, A., Angell, A. D. R., Jepson, C. A., Yeaman, S. J., and Hassall, D. G. (1996) *Atherosclerosis 120*, 135−145.
27. Rothblat, G. H., Llera-Moya, M. D. L., Atger, V., Kellner-Weibel, G., Williams, D. L., and Phillips, M. C. (1999) *J. Lipid Res. 40*, 781−795.
28. Costet, P., Yi, L., Wang, N., and Tall, A. R. (2000) *J. Biol. Chem. 275*, 28240−28245.
29. Han, J., Nicholson, A. C., Zhou, X., Feng, J., Gotto, J., and Hajjar, D. P. (2001) *J. Biol. Chem.*, in press.

BI010323N